Ancora, D., Di Battista, D., Vidal, A. M., Avtzi, S., Zacharakis, G., & Bassi, A. (2021, March). Hidden projection tomography via phase retrieval algorithm. In Quantitative Phase Imaging VII (Vol. 11653, p. 116530P). International Society for Optics and Photonics.

https://doi.org/10.1117/12.2582996

Hidden projection tomography via phase retrieval algorithm

Daniele Ancora[1*], Diego Di Battista[2], Asier Marcos Vidal[3], Stella Avtzi[2,4], Giannis Zacharakis[2], and Andrea Bassi[1,5]

[1]Dipartimento di Fisica, Politecnico di Milano, Piazza Leonardo da Vinci 32, 20133 Milano, Italy
[2]Institute of Electronic Structure and Laser, Foundation for Research and Technology-Hellas, N. Plastira 100, 70013 Heraklion, Greece
[3]Department of Bioengineering and Aerospace Engineering, Universidad Carlos III de Madrid, 28911 Leganés, Spain
[4]Institut de Ciències Fotòniques, Barcelona Institute of Science and Technology, Av. Carl Friedrich Gauss, 3, 08860 Castelldefels, Spain
[5]Istituto di Fotonica e Nanotecnologie, Consiglio Nazionale delle Ricerche, Piazza Leonardo da Vinci 32, 20133 Milano, Italy

ABSTRACT

The reconstruction of an object hidden behind a scattering curtain is a modern topic in the field of imaging, which has stimulated an active scientific production over the past few years. However, most of the work done in the field was in addressing the reconstruction of a bi-dimensional object. Here, instead, we tackle the reconstruction of a three-dimensional fluorescent sample hidden behind an opaque layer. To do so, we show that the auto-correlation operation well behave in projection tomography, letting us to reconstruct a three-dimensional auto-correlation of the object. By having access to such information, it is possible to implement a phase retrieval algorithm to roll back to the actual reconstruction of the specimen.

Keywords: Phase retrieval, hidden imaging, computed tomography, fluorescence imaging, auto-correlation, GPU computing.

1. INTRODUCTION

The field of computed tomography has experienced numerous improvements over the last decade, mainly concerning algorithm developments and boosted by the usage of GPU computing paradigm. In this proceeding, we describe a new finding that enables the reconstruction of a hidden specimen behind a scattering curtain. Up to now, hidden imaging was mostly accomplished by reconstructing two-dimensional object,[1,2] and only recently a first attempt with a simple object constituted by dots[3] was carried out in a 3D sample. Here, we discuss a tomographic approach for hidden reconstructions. By combining results from the field of computed tomography (CT) and those of hidden imaging, we address the problem of the reconstruction of an three-dimensional specimen out-of-sight and without any optics. We take inspiration by alignment-free projection tomography enabled via the computation of the auto-correlation sinogram.[4] It is possible, to change the order between the auto-correlation and the projection operators, so that the inversion of the auto-correlation sinogram produces the three-dimensional auto-correlation of the object. By doing so, the object is formed free from any alignment issue[5] and without any prior knowledge of the spatial distribution of the object that we are interested to image.

2. MATERIALS AND METHODS

2.1 The auto-correlation of a speckle pattern

In the following, we describe the theoretical framework under which is possible to accomplish hidden tomography. Let us assume that we have a fluorescent specimen hidden behind layer of diffusing material (such for example a ground glass diffuser). Furthermore, we assume that the measurement falls within the memory effect conditions.[1] If that is the case, the light emitted by the object propagates through the diffuser and gives rise to a speckle pattern S_φ (supposing a given object orientation at an angle φ). Since we assumed that the memory effect holds,

*For the correspondence email to: daniele.ancora@polimi.it

the point spread function of the system (that would look like a random speckle pattern too) is isoplanatic, and we can write:

$$S_\varphi = O_\varphi * \mathrm{PSF}_\varphi, \tag{1}$$

being O_φ the object projection at angle φ and subject to a point-spread-function PSF_φ. In this representation, the random diffuser acts as a normal optical element having a very complicated PSF. The PSF of the system, in this case, also resembles a speckle pattern. If we are able to measure the response of the system PSF_φ, we could reconstruct the object O_φ via a deconvolution approach.[6] However, to have access to such information we should estimate it somehow, by accessing the other side of the diffuser. Here, instead, we consider the case in which it is not possible to measure the PSF_φ by any mean. To be able to reconstruct the object, we should exploit the statistical properties of the speckle patterns. If the random medium is truly disordered, the random arrangements of intensity peaks satisfy the auto-correlation property:

$$\mathrm{PSF}_\varphi \star \mathrm{PSF}_\varphi = \delta. \tag{2}$$

This means that there is no ordering in the speckle produced by a point source. Thanks to this, if we examine the auto-correlation of the speckle produced by hiding the specimen:

$$\begin{aligned} S_\varphi \star S_\varphi &= (O_\varphi * \mathrm{PSF}_\varphi) \star (O_\varphi * \mathrm{PSF}_\varphi) \\ &= (O_\varphi \star O_\varphi) * (\mathrm{PSF}_\varphi \star \mathrm{PSF}_\varphi) = O_\varphi \star O_\varphi. \end{aligned} \tag{3}$$

we are left with the auto-correlation of the object, as the disorder has helped regain a property otherwise lost. It appears clear that by computing the auto-correlation of such S_φ, we are effectively calculating the same quantity as if the object was imaged directly. For this reason, we can talk about the random media as being an auto-correlation lens. There is a linear magnification rule that holds in this kind of imaging, and it is directly related to the distances between the object and the diffuser (d_2) and between the diffuser and the camera (d_1):

$$M = \frac{d_1}{d_2}. \tag{4}$$

This implies that we can magnify as we move the camera further away from the diffuser. However, we should find a compromise between magnification and speckle statistics. If the number of speckles collected in the image is not statistically sufficient, the Eq. 2 is not necessarily satisfied.

2.2 The auto-correlation sinogram and its inversion

Let us assume that what discussed in the previous section holds at any rotation of the object, where the PSF_φ may vary but the memory effect of Eq.2 still remains satisfied. As a consequence, measuring the patterns S_φ during its complete rotation leaves us with a stack of speckles that cannot be directly inverted. Instead, we process them by calculating each time the auto-correlation, building in such a way the auto-correlation sinogram:

$$\chi_\varphi = S_\varphi \star S_\varphi. \tag{5}$$

It is possible to prove that the sinogram χ_φ can be inverted by using projection theorems similarly to what done in computed tomography.[5,7] Algorithm such as inverse radon transform or algebraic methods[8] let us accomplish the sinogram inversion and enables the reconstruction of the three-dimensional auto-correlation of the specimen. In this representation, if we call the projection that gives rise to the sinogram as $\mathcal{P}$, we represent its inversion as the operator $\mathcal{P}^{-1}$. In the present work, we use the simultaneous iterative reconstruction technique (SIRT) to accomplish the inversion of the auto-correlation sinogram.[8] We have found this to behave well for our purpose, however we do not exclude that other techniques may lead to better results. The finalization of this inversion, leads to the reconstruction of the tomographic auto-correlation that we call $\mathcal{X} = \mathcal{P}^{-1}\{\chi_\varphi\}$.

2.3 Object reconstruction via phase retrieval

Once the estimation of the object auto-correlation is formed, we need to calculate the the corresponding Fourier modulus by making use of the Wiener-Kinchin power spectrum relation. In practice, the Fourier modulus can be calculated as:

$$\mathcal{M} \equiv \|\mathcal{F}\{\mathcal{O}\}\| = \sqrt{\mathcal{F}\{\mathcal{X}\}}, \tag{6}$$

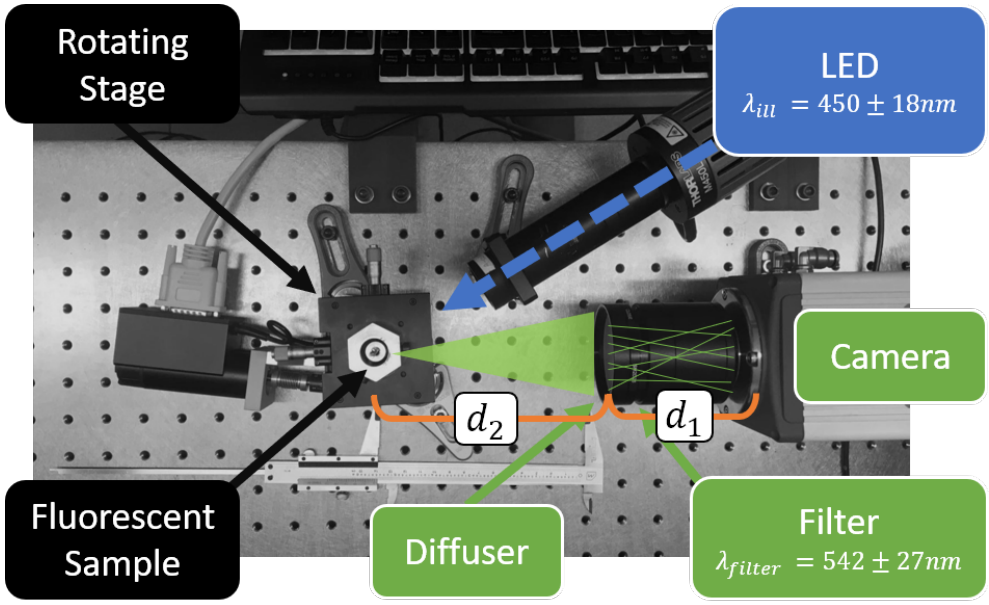

Figure 1. Imaging setup used for the experiment. The fluorescent sample is hold in place by a rotating stage, which permits the full rotation of the specimen. A blue LED source excites the fluorescent emission, that propagates isotropically in every direction. A fraction of the signal propagates through the diffuser (Thorlabs) and it is filtered by a band-pass filter placed in front of the camera. In this way, the intensity recorded by the sensor is speckled and does not resemble the original object.

where $\mathcal{O}(\boldsymbol{x})$ is the actual object in the 3D space. We have the reconstruction of the modulus $\mathcal{M}$, to reconstruct the object we only miss the phase information. In our case, we have a strong prior that we can exploit to ease the process, i.e. the reconstruction of a fluorescent object must be real and positive by definition. This is enough to let the three-dimensional phase retrieval (PR) process to converge into a unique solution.[9] Starting with the modulus, we implement a standard PR algorithm that seek for the phase to associate to, that leads towards a real and positive object.

In the following, we describes the steps to implement the error reduction algorithm and the hybrid input-output iterative methods. Both share the three initial steps, only the fourth changes:

1. First, we perform a Fourier transform of the current object estimation $\mathcal{O}_i$:

$$\mathcal{F}\{\mathcal{O}_i\} = \|\mathcal{F}\{\mathcal{O}_i\}\|e^{i\Phi_i}. \tag{7}$$

2. In the second step, we insert the measured modulus $\mathcal{M}$ in the previous equation, by replacing the previously obtained one:

$$\mathcal{G}_i' = \mathcal{M}\frac{\mathcal{F}\{\mathcal{O}_i\}}{\|\mathcal{F}\{\mathcal{O}_i\}\|} = \mathcal{M}e^{i\Phi_i}. \tag{8}$$

3. The third operation is a simple inverse Fourier transform of the $\mathcal{G}_i'$, returning back to the object space:

$$\mathcal{O}_i' = \mathcal{F}^{-1}\{\mathcal{G}_i'\}. \tag{9}$$

   Here, we are not guarantee that $\mathcal{O}_i'$ is real and positive.

4. This is the most important step, in which we apply the object constraints. It is also the only difference between the ER and HIO implementations. We define the region γ as the voxels in the volume where the

$\mathcal{O}_i$ is not real an positive. For the ER, the object $\mathcal{O}_{i+1}$ is formed by setting to zero the values of the voxels in γ:

$$\mathcal{O}_{i+1} = \begin{cases} \mathcal{O}'_i & \text{if } \boldsymbol{x} \notin \gamma \\ 0 & \text{if } \boldsymbol{x} \in \gamma. \end{cases} \tag{10}$$

For the HIO, instead, we introduce a feedback term β that acts only in the region γ that weights the previous estimation:

$$\mathcal{O}_{i+1} = \begin{cases} \mathcal{O}'_i & \text{if } \boldsymbol{x} \notin \gamma \\ \mathcal{O}_i - \beta\mathcal{O}'_i & \text{if } \boldsymbol{x} \in \gamma. \end{cases} \tag{11}$$

Typically, in hidden imaging based on auto-correlation inversion, one starts with HIO iterations that guarantee rapid convergence, and then finalizes with a few ER iterations that suppress the noise. At the end of those iterations, we are left with the three-dimensional estimation of the object that was hidden behind the optical diffuser.

3. RESULTS AND CONCLUSIONS

In the previous section, we have defined the algorithmic strategy to deal with tomographic reconstruction in hidden imaging setups. Due to its robust design, the setup is actually very simple and it is illustrated in figure 1. A fluorescent sample (Microscopy Education FluorRef-Green) resembling a small lambda shape, is kept in place by mounting it on a rotating stage. The fluorescence is stimulated by an LED source (Thorlabs, M450LP1, $\lambda_{\text{ill}} = 450 \pm 18nm$), and propagates isotropically. A portion of this light trespasses a ground glass diffuser (Thorlabs, grit 1200) that is placed in front of the camera (Hamamatsu ORCA flash 4.0). Before it reaches the sensor, the light is further filtered by a band-pass filter (Brightline, $542/27nm$) to enhance the speckle contrast. As soon as the speckle pattern S_φ is recorded, we rotate the specimen by an angular step of 2° and we repeat the

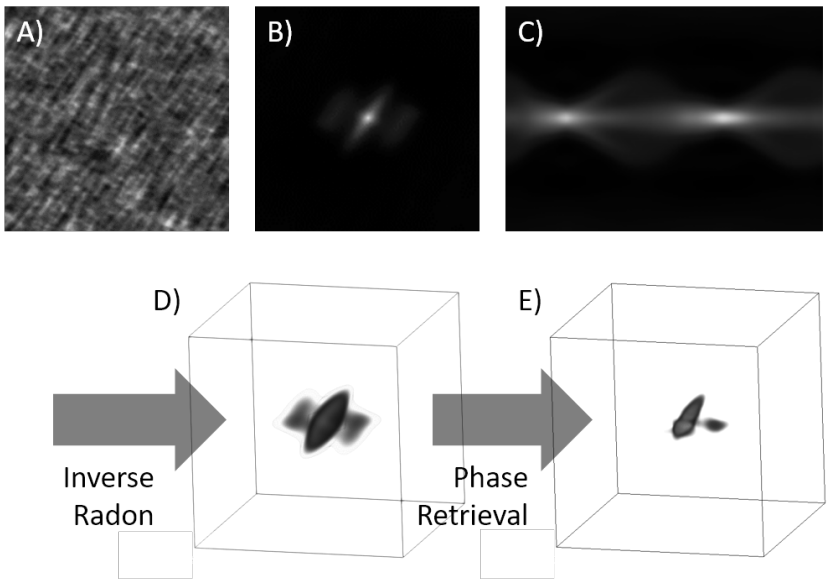

Figure 2. Schematics of the pipeline for the data processing. The camera records a speckle pattern similar to the one in panel A). By computing its auto-correlation, we obtain the image in figure B), which in case of memory effect regime, resembles the auto-correlation of the object that we are interested in. By rotating the sample and calculating the auto-correlation of each speckle acquired, we form the auto-correlation sinogram C). The inversion of such sinogram, leaves us with the reconstruction of the three-dimensional auto-correlation of the sample D). By running a phase retrieval algorithm on this volume, it is possible to reveal the object that was secreted behind the diffuser E).

measurement until we have completed a full rotation. The speckle patter obtained at $\varphi = 0°$ is reported in Fig. 2A. Based on this acquisition, we compute its auto-correlation (Fig. 2B). By stacking all the auto-correlations obtained at every angles, we form the auto-correlation sinogram χ_φ in Fig. 2C. As we can notice, the sinogram rotates around its center by definition and it does not require any alignment procedure.[7] We invert the χ_φ via a SIRT algorithm, that gives rise to the reconstruction of the auto-correlation of the whole specimen rendered in Fig. 2D. By definition, the $\mathcal{X}$ is also centered. As described in Sec. 2.3, we use it to estimate the modulus of the Fourier transform and we recover the phase by running 1000 iterations of HIO and 500 iterations of ER.

This process leads to the result rendered in Fig. 2E. The reconstruction is faithful to the original, and it is reconstructed in a random location in space due to non trivial ambiguities in the auto-correlation inversion. However, it is consistent and all the features are appropriately aligned by definition.[5] In this report, we demonstrated how with a simple optical setup with no optics involved it is possible to reconstruction an object hidden behind a turbid wall. The tomographic capabilities are guaranteed by the theoretical framework developed for the auto-correlations analysis[4] and it is a promising approach that can be applied also in conventional imaging techniques. Furthermore, by characterizing the effect of a given PSF in the auto-correlation space, we may include also a deconvolution approach in the reconstruction pipeline.[10] We are committed to develop further auto-correlation based reconstructions in computed tomography, since they show promising performances in terms of the quality of the results and are flexible under hidden and direct measurement conditions.

ACKNOWLEDGMENTS

The research has received support from the European Union's Horizon 2020 research and innovation programme under the Marie Sklodowska-Curie project (H2020-MSCA-IF-2017, project acronym: HI-PHRET, G.A. 799230) and under H2020 Laserlab Europe V (G.A. 871124). The authors thank Prof. Antonio Pifferi for the scientific and logistic support.

REFERENCES

[1] Bertolotti, J., Van Putten, E. G., Blum, C., Lagendijk, A., Vos, W. L., and Mosk, A. P., "Non-invasive imaging through opaque scattering layers," *Nature* **491**(7423), 232 (2012).

[2] Katz, O., Heidmann, P., Fink, M., and Gigan, S., "Non-invasive single-shot imaging through scattering layers and around corners via speckle correlations," *Nature photonics* **8**(10), 784 (2014).

[3] Okamoto, Y., Horisaki, R., and Tanida, J., "Noninvasive three-dimensional imaging through scattering media by three-dimensional speckle correlation," *Optics letters* **44**(10), 2526–2529 (2019).

[4] Ancora, D., Di Battista, D., Giasafaki, G., Psycharakis, S. E., Liapis, E., Ripoll, J., and Zacharakis, G., "Phase-retrieved tomography enables mesoscopic imaging of opaque tumor spheroids," *Scientific reports* **7**(1), 11854 (2017).

[5] Ancora, D., Di Battista, D., Vidal, A. M., Avtzi, S., Zacharakis, G., and Bassi, A., "Hidden phase-retrieved fluorescence tomography," *Optics letters* **45**(8), 2191–2194 (2020).

[6] Wu, T., Dong, J., and Gigan, S., "Non-invasive single-shot recovery of a point-spread function of a memory effect based scattering imaging system," *Optics Letters* **45**(19), 5397–5400 (2020).

[7] Ancora, D., Di Battista, D., Giasafaki, G., Psycharakis, S. E., Liapis, E., Ripoll, J., and Zacharakis, G., "Optical projection tomography via phase retrieval algorithms," *Methods* **136**, 81 – 89 (2018). Methods in Quantitative Phase Imaging in Life Science.

[8] Kak, A. C., Slaney, M., and Wang, G., "Principles of computerized tomographic imaging," *Medical Physics* **29**(1), 107–107 (2002).

[9] Shechtman, Y., Eldar, Y. C., Cohen, O., Chapman, H. N., Miao, J., and Segev, M., "Phase retrieval with application to optical imaging: a contemporary overview," *IEEE signal processing magazine* **32**(3), 87–109 (2015).

[10] Ancora, D. and Bassi, A., "Deconvolved image restoration from auto-correlations," *IEEE Transactions on Image Processing* **30**, 1332–1341 (2020).